Available online at www.sciencedirect.com
SCIENCE DIRECT
Journal of Photochemistry and Photobiology A: Chemistry 176 (2005) 155–161
Journal of Photochemistry and Photobiology A:Chemistry
www.elsevier.com/locate/jphotochem

Kinetic and mechanistic study of the reactions of OH with IBr and HOI

Véronique Riffault [a], Yuri Bedjanian [a,*], Gilles Poulet [b]

[a] *Laboratoire de Combustion et Systèmes Réactifs, CNRS and Université d'Orléans, 45071 Orléans Cedex 2, France*
[b] *Laboratoire de Physique et Chimie de l'Environnement, CNRS and Université d'Orléans, 45071 Orléans Cedex 2, France*

Available online 20 October 2005

Abstract

The kinetics and mechanism of the reactions of OH radicals with IBr and HOI have been studied using the mass spectrometric discharge-flow method at 320 K and at a total pressure of 1 Torr of Helium. The rate constant of the reaction OH + IBr → products (1) was measured under pseudo-first order conditions either in excess of IBr or in excess of OH radicals: $k_1 = (1.4 \pm 0.4) \times 10^{-10}$ cm^3 molecule^{-1} s^{-1}. Both HOI and HOBr were detected as products of reaction (1) and the branching ratios 0.84 ± 0.07 and 0.14 ± 0.05, respectively, were found for the channels forming these species. For the reaction OH + HOI → products (2) the total rate constant was determined from the kinetics of HOI consumption in excess of OH radicals: $k_2 = (5.0 \pm 1.2) \times 10^{-12}$ cm^3 molecule^{-1} s^{-1}.

Keywords: Reaction; Kinetics; Rate constant; OH; HOI; IBr

1. Introduction

Elementary reactions of many halogen containing species have received a lot of attention during the last three decades, mainly due to their great importance for atmospheric chemistry. If the reactions of OH radicals with halogen molecules X_2 (X = Cl, Br, I) are not relevant for atmospheric chemistry, they have been studied intensively (see evaluations [1,2] and references therein) since these reactions are often used as sources for HOX species in laboratory studies of the halogen chemistry. Reactions of OH radicals with dihalogen molecules XY (X, Y = Cl, Br, I) are of additional interest since they can proceed via multiple reaction pathways:

$$\begin{aligned} OH + XY &\rightarrow X + HOY \\ &\rightarrow Y + HOX \\ &\rightarrow YO + HX \\ &\rightarrow XO + HY \end{aligned}$$

HX and HY forming channels are disfavored as they require a complicated mechanism including HX and HY elimination from a cyclic four-center transition state. The measurements of the partitioning between HOX and HOY formation is very interesting either for practical or theoretical studies in order to elucidate the reaction mechanism. To our knowledge, the data available for OH + XY reactions are very scarce. Loewenstein and Anderson, using discharge flow reactor combined with resonance fluorescence detection system, measured the rate constant for the OH + BrCl reaction [3] and carried out a kinetic and mechanistic study of the OH + ICl reaction [4]. Mechanistic information on the OH + BrCl reaction was reported by Kukui et al. [5].

The present study gives the results of a kinetic and mechanistic study of the reaction of OH radical with IBr, another dihalogen molecule, at $T = 320$ K:

$$OH + IBr \rightarrow \text{products} \quad (1)$$

In addition, the reaction of OH radicals with HOI, one of the products of reaction (1), has been also studied and results are reported for this reaction:

$$OH + HOI \rightarrow \text{products} \quad (2)$$

2. Experimental

Experiments were carried out in a discharge flow reactor using a modulated molecular beam mass spectrometer as the detection method. The main reactor, shown in Fig. 1 along with the movable injector for the reactants, consisted of a Pyrex tube (45 cm length and 2.4 cm i.d.) with a jacket for the thermostated liquid circulation. The walls of both the reactor and the injector were coated with halocarbon wax to minimize the heteroge-

* Corresponding author. Tel.: +33 238255474; fax: +33 238696004.
E-mail address: bedjanian@cnrs-orleans.fr (Y. Bedjanian).

1010-6030/$ – see front matter © 2005 Elsevier B.V. All rights reserved.
doi:10.1016/j.jphotochem.2005.09.002

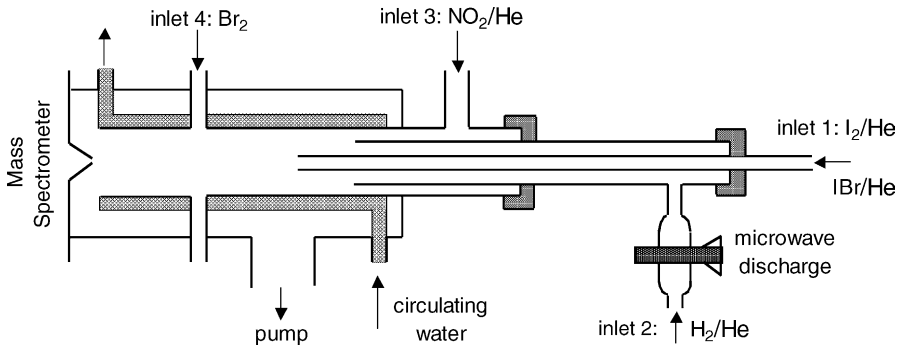

Fig. 1. Diagram of the flow reactor used.

neous loss of active species. All experiments were conducted at 1 Torr total pressure, Helium being used as the carrier gas, and at $T = 320$ K, the reactor was slightly heated in order to minimize the possible heterogeneous complications due to the sticky behaviour of iodine containing species.

The fast reaction of hydrogen atoms with NO_2 was used as the source of OH radicals, H atoms being produced in a microwave discharge of H_2/He mixture:

$$H + NO_2 \rightarrow OH + NO \quad (3)$$

$k_3 = 1.4 \times 10^{-10}$ cm^3 molecule^{-1} s^{-1} [1] (all rate constants are given at $T = 320$ K, unless otherwise specified). OH radicals were detected at their parent peaks at $m/e = 17$ (OH^+). These signals were corrected for contributions from H_2O due to its fragmentation in the ion source (operated at 25–30 eV), H_2O being formed in the reactions of disproportionation of OH:

$$OH + OH \rightarrow O + H_2O \quad (4)$$

$k_4 = 1.4 \times 10^{-12}$ cm^3 molecule^{-1} s^{-1} [2]. These corrections could be easily done from the simultaneous detection of the signals of H_2O at $m/e = 17$ and 18. In another method, OH were detected as $HOBr^+$ ($m/e = 96/98$) after scavenging by an excess of Br_2 (added at the end of the reactor through inlet 4, located 5 cm upstream of the sampling cone) via reaction (5):

$$OH + Br_2 \rightarrow Br + HOBr \quad (5)$$

$k_5 = 4.2 \times 10^{-11}$ cm^3 molecule^{-1} s^{-1} [2]. This procedure of OH chemical conversion to HOBr was also used for the measurements of the absolute concentrations of the radicals: $[OH] = [HOBr] = \Delta[Br_2]$. Thus, OH concentrations were determined from the consumed fraction of Br_2 ($\Delta[Br_2]$). Besides, this method allowed for the determination of the absolute concentrations of HOBr. $[Br_2]$ was determined from the measured flow rate of known Br_2/He mixtures. The possible influence of secondary chemistry in this detection method and on the OH calibration procedure was discussed in details in previous papers [6,7]. All other species used in the study were detected at their parent peaks.

Molecular iodine and IBr were introduced into the reactor by flowing helium through a column containing I_2 or IBr crystals. With an excess of molecular iodine over Br atoms, reaction (6) was used for the determination of the absolute concentrations of I_2 and IBr molecules ($[Br]_0 = \Delta[I_2] = [IBr]$):

$$Br + I_2 \rightarrow I + IBr \quad (6)$$

$k_6 = 1.2 \times 10^{-10}$ cm^3 molecule^{-1} s^{-1} ($T = 298$ K) [8]. Br atoms were generated in a microwave discharge of Br_2/He mixtures. The absolute concentrations of Br atoms were determined from the measurements of the fraction of Br_2 dissociated in the microwave discharge: $[Br]_0 = 2\Delta[Br_2]$.

HOI molecules were formed from the fast reaction of OH radicals with I_2:

$$OH + I_2 \rightarrow I + HOI \quad (7)$$

$k_7 = 2.1 \times 10^{-10}$ cm^3 molecule^{-1} s^{-1} [2]. This chemical conversion of OH to HOI by an excess of I_2 was also used for the determination of the absolute concentrations of HOI: $[HOI] = [OH]_0 = \Delta[I_2]$.

The purities of the gases used in the study were as follows: He >99.9995% (Alphagaz) was passed through a liquid nitrogen trap; H_2 >99.998% (Alphagaz); Br_2 >99.99% (Aldrich); NO_2 >99% (Alphagaz); I_2 >99.999% (Aldrich); IBr 98% (Aldrich).

3. Results

3.1. Reaction OH + IBr (1): rate constant measurement

Two series of experiments were performed: in the first one, the rate constant of reaction (1) was measured by monitoring the IBr consumption kinetics in excess of OH radicals, and in the second one, OH decays were monitored using an excess of IBr. A similar configuration for the introduction of the reactants into the reactor was used in both series of experiments (see Fig. 1). IBr was introduced through the central tube of the movable injector and OH radicals were formed in the reactor via reaction (3), H atoms generated in a microwave discharge being introduced through inlet 2 and NO_2 through the reactor sidearm (inlet 3).

In the experiments carried out with an excess of OH radicals over IBr, the initial concentrations of IBr were in the range $(0.4–1.2) \times 10^{12}$ molecule cm^{-3}; the concentration of excess OH radicals was varied between 0.5 and 5.5×10^{12} molecule cm^{-3}. Flow velocity in the reactor was in the range 1700–2030 cm s^{-1}. The consumption of the excess reactant, OH radicals, was observed in all experiments and reached up to 60% in a few kinetic runs. This consumption of

OH radicals was mainly due to their reaction with IBr (due to slight excess of [OH] over [IBr]), but also to the secondary reaction of OH with HOI (HOI being a product of reaction (1), see reaction (2)).

Heterogeneous loss (reaction (8)) and self-reaction of OH radicals (4) also contributed to OH decays:

$$OH + \text{wall} \rightarrow \text{loss} \quad (8)$$

$k_8 = (10 \pm 3)\,s^{-1}$ (this work). The rate constant k_1 was derived from a numerical simulation of the IBr decays in reaction (1), using the observed [OH] temporal profiles. The possible IBr consumption in secondary reaction (9) was negligible under the experimental conditions of this study:

$$Br + IBr \rightarrow I + Br_2 \quad (9)$$

$k_9 = 2.7 \times 10^{-11}\,cm^3\,molecule^{-1}\,s^{-1}$ [9]. The results are presented in Fig. 2 showing the dependence of the pseudo-first order rate constants, $k_1' = k_1 \times [OH]$, as a function of OH concentration (circle data). The values of k_1' were corrected for axial and radial diffusion of IBr [10]. The diffusion coefficient of IBr in He was calculated from that of Xe in He [11]. Typical corrections were within 10%.

In the second series of experiments, the rate constant of reaction (1) was determined from the kinetics of OH consumption in excess of IBr. Initial concentrations of the reactants were: $[OH]_0 = (0.3–0.9) \times 10^{11}$ and $[IBr]_0 = (1.4–4.9) \times 10^{12}$ molecule cm^{-3}.

In order to take into account for the OH consumption in reactions other than reaction (1), the rate coefficient of reaction (1) was also calculated via numerical simulation of the OH kinetics using the observed temporal profiles of excess IBr concentration (consumption of 10–50% of $[IBr]_0$ was observed) and a simple kinetic mechanism including reactions (1), (2), (4) and (8). The results are presented in Fig. 2 as the dependence of $k_1' = k_1 \times$ [IBr]on the concentration of IBr molecules (square data).

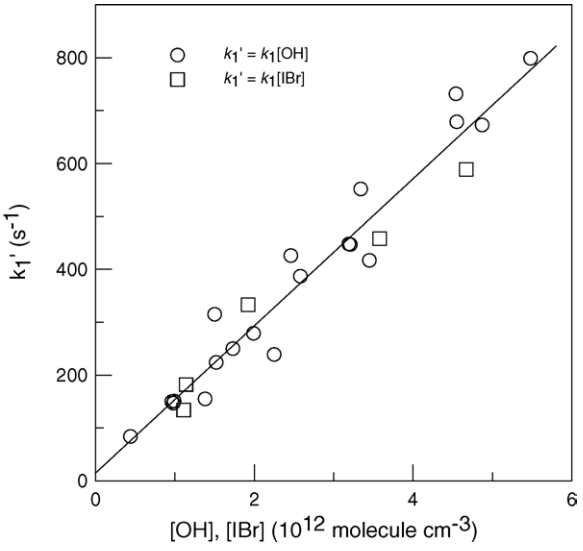

Fig. 2. Reaction OH + IBr → products (1): pseudo-first order plots obtained from IBr and OH decay kinetics in excess of OH and IBr, respectively.

The value of k_1 which can be derived from the slope of the linear least square fit to all experimental data presented in Fig. 2 is: $k_1 = (1.39 \pm 0.07) \times 10^{-10}\,cm^3\,molecule^{-1}\,s^{-1}$, with 1σ statistical uncertainty. Finally, the recommended value of k_1 from this study is:

$$k_1 = (1.4 \pm 0.4) \times 10^{-10}\,cm^3\,molecule^{-1}\,s^{-1} \quad (T = 320\,K)$$

The uncertainty on k_1 represents the combination of statistical and estimated systematic errors. The estimated systematic uncertainties include ±5% for flow meter calibrations, ±3% for pressure measurements and ±20% for measurements of the absolute concentrations of the species and for the procedure employed for the determination of k_1. Combining these uncertainties in quadrature and adding 1σ statistical uncertainty yields the quoted near 30% uncertainty on k_1.

3.2. Reaction OH + IBr (1): product study

The reaction between IBr and OH radicals may proceed following several potential channels:

$$OH + IBr \rightarrow Br + HOI \quad \Delta H = -(35.8 \pm 6.0)\,kJ\,mol^{-1} \quad (1a)$$

$$OH + IBr \rightarrow I + HOBr \quad \Delta H = -(31.8 \pm 1.6)\,kJ\,mol^{-1} \quad (1b)$$

$$OH + IBr \rightarrow IO + HBr \quad \Delta H = 1.5 \pm 5.6\,kJ\,mol^{-1} \quad (1c)$$

$$OH + IBr \rightarrow BrO + HI \quad \Delta H = 74.6 \pm 2.3\,kJ\,mol^{-1} \quad (1d)$$

The thermochemical data used for the calculations of ΔH are from reference [1] (for $T = 298$ K). Channel (1d) is too endothermic to proceed with a rate constant as high as the measured one. The near thermoneutral channel (1c) also seems to be unlikely, since would imply a complex rearrangement of a four-center transition state.

The mechanistic study of reaction (1) was carried out using an excess of IBr over OH radicals and was based on the measurements of the concentrations of the reaction products, HOI and HOBr, formed in reactions (1a) and (1b), respectively, as a function of the consumed concentration of OH radicals. In order to avoid additional systematic errors due to the absolute calibration of the species involved, a relative method was used to determine the initial concentrations of OH radicals. In fact, $[OH]_0$ could be related to the intensities of mass spectrometric signals of the reaction products at $m/e = 144$ (HOI^+) and 96/98 ($HOBr^+$) by means of chemical conversion of OH to HOI and HOBr in the reactions with excess I_2 and Br_2, respectively. Thus, no absolute OH concentrations measurements were needed and, in the series of experiments, OH was successfully titrated with I_2 to express

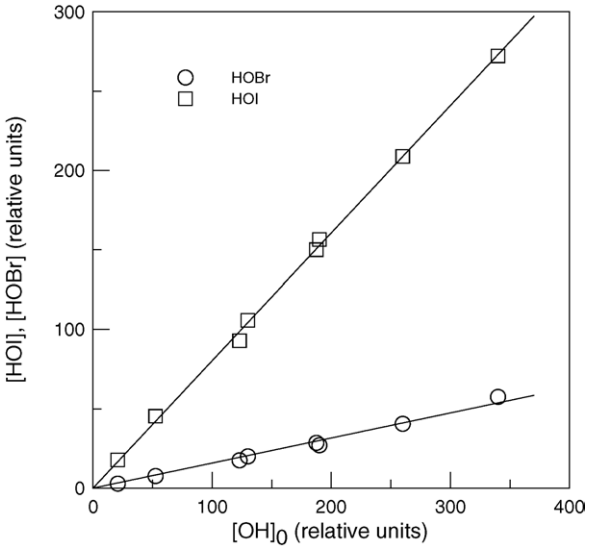

Fig. 3. Reaction OH + IBr → products (1): concentrations of HOBr and HOI formed in reaction (1) as a function of consumed concentration of OH radicals.

$[OH]_0$ in the units of HOI signal, with Br_2 to express the $[OH]_0$ in the units of HOBr signal and with IBr to detect HOI and HOBr formed in reaction (1). In order to avoid possible OH consumption in secondary reactions, rather high concentrations of Br_2, I_2 and IBr (near 10^{14} molecule cm^{-3}) were used in these experiments. Under theses conditions, OH radicals with initial concentration in the range 1.0×10^{12}–1.6×10^{13} molecule cm^{-3} were rapidly transformed into the observed products.

The observed concentrations of HOI and HOBr are plotted in Fig. 3 as a function of the consumed concentration of OH radicals. The linear fit to the presented results provides the calculation of the branching ratios for the HOBr and HOI forming pathways of reaction (1):

$$[HOBr]_{formed}/[OH]_{consumed} = 0.16 \pm 0.02$$

$$[HOI]_{formed}/[OH]_{consumed} = 0.80 \pm 0.03$$

(the quoted errors are statistical 2σ uncertainties).

3.3. Reaction OH + IBr (1): relative measurements

In this series of experiments, the rate constant of reaction (1) was measured using the reaction (5) of OH with Br_2 as the reference. The approach used in this relative study consisted of the titration of the initial concentration of OH, $[OH]_0$, by a mixture of excess IBr and Br_2 and the measurements of the HOBr and HOI yields as a function of the $[Br_2]/[IBr]$ ratio. The concentrations of HOI and HOBr are derived from the simple reaction system:

$$OH + IBr \rightarrow Br + HOI \quad (1a)$$

$$OH + IBr \rightarrow I + HOBr \quad (1b)$$

$$OH + Br_2 \rightarrow Br + HOBr \quad (5)$$

Thus, the concentration of HOI is defined by the fraction of $[OH]_0$ reacting with IBr via reaction (1a):

$$[HOI] = \frac{k_{1a}[IBr]}{k_5[Br_2] + k_1[IBr]}[OH]_0$$

This expression can be rewritten as follows:

$$\frac{[OH]_0}{[HOI]} = \frac{k_1}{k_{1a}} + \frac{k_5}{k_{1a}} \times \frac{[Br_2]}{[IBr]} \quad (I)$$

Similar considerations for HOBr lead to the following expressions:

$$[HOBr] = \frac{k_5[Br_2] + k_{1b}[IBr]}{k_5[Br_2] + k_1[IBr]}[OH]_0,$$

$$\frac{[HOBr]}{[OH]_0 - [HOBr]} = \frac{k_{1b}}{k_{1a}} + \frac{k_5}{k_{1a}} \times \frac{[Br_2]}{[IBr]} \quad (II)$$

Finally, plotting the ratios $[OH]_0/[HOI]$ and $[HOBr]/([OH]_0-[HOBr])$ as a function of the $[Br_2]/[IBr]$ ratio, the rate constant ratios k_1/k_{1a}, k_{1b}/k_{1a} and k_5/k_{1a} can be derived from the intercepts and slopes of the respective straight lines according to expressions (I) and (II).

The experimental results obtained using this approach are shown in Fig. 4. The intercept of the straight line corresponding to HOI (circle data) leads to: $k_1/k_{1a} = 1.13$. This gives the following value for the branching ratio of the HOI forming pathway of reaction (1):

$$\frac{k_{1a}}{k_1} = 0.88 \pm 0.03\,(2\sigma)$$

Similarly, the value $k_{1b}/k_{1a} = 0.14$ is determined from the intercept of the straight line fitting HOBr data (squares in Fig. 4). Thus, the branching ratio for channel (1b) can be easily obtained:

$$\frac{k_{1b}}{k_1} = 0.12 \pm 0.05\,(2\sigma)$$

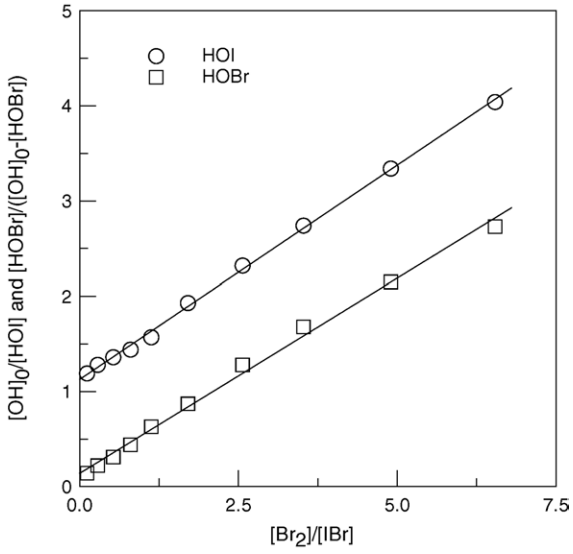

Fig. 4. Determination of k_1/k_{1a}, k_{1b}/k_{1a} and k_5/k_{1a} from the experimental data according to expressions (I) and (II) (see text).

One can note the good agreement between the results obtained in this series of relative experiments and in the direct measurements of the products concentrations reported above: 0.16 ± 0.03 and 0.80 ± 0.03 for k_{1b}/k_1 and k_{1a}/k_1, respectively. Finally, the mean values of k_{1a}/k_1 and k_{1b}/k_1 from the two series of experiments are recommended from this study ($T = 320$ K):

$$\frac{k_{1a}}{k_1} = 0.84 \pm 0.07$$

$$\frac{k_{1b}}{k_1} = 0.14 \pm 0.05$$

Additional information can be derived from the slopes of the straight lines obtained in Fig. 4. As expected, they have similar (within 10%) slopes corresponding to k_5/k_{1a} ratio: 0.45 ± 0.02 (2σ) and 0.41 ± 0.02 (2σ), respectively from the HOI and HOBr data. Taking the mean value of $k_5/k_{1a} = 0.43 \pm 0.04$, and combining it with $k_{1a}/k_1 = 0.84 \pm 0.07$ determined above, it comes: $k_5/k_1 = 0.36 \pm 0.06$. Thus, the value of the total rate constant of reaction (1) can be determined relatively to k_5. The temperature dependence of the rate constant of the $OH + Br_2$ reaction is well established, considering the excellent agreement between the two most recent measurements: $k_5 = (1.98 \pm 0.51) \times 10^{-11} \exp[(238 \pm 70)/T]$ [12] and $k_{12} = (1.8 \pm 0.3) \times 10^{-11} \exp[(235 \pm 50)/T]$ cm^3 molecule^{-1} s^{-1} [7]. The value of k_5 based on these expressions and other literature data is $k_5 = 2.0 \times 10^{-11} \exp[(240 \pm 150)/T]$ cm^3 molecule^{-1} s^{-1} [2], which gives at $T = 320$ K: $k_5 = (4.2 \pm 0.5) \times 10^{-11}$ cm^3 molecule^{-1} s^{-1}. Combining this value with $k_5/k_1 = 0.36 \pm 0.06$, the value of k_1 can be calculated: $k_1 = (1.2 \pm 0.6) \times 10^{-10}$ cm^3 molecule^{-1} s^{-1}. This value is in excellent agreement with that obtained above in the absolute measurements of k_1.

The experimental data obtained in this study for two reaction products (HOI and HOBr) give self-consistent results either for the branching ratios of the channels forming these species or for the total value of the rate constant for reaction (1).

3.4. Reaction OH + HOI (2)

In this series of experiments, the rate constant of reaction (2) was derived from the kinetics of HOI consumption monitored using an excess of OH radicals. HOI molecules were produced directly in the reactor from the reaction of excess OH radicals with molecular iodine. I_2 was introduced into the reactor (see Fig. 1) through the central tube of the movable injector (inlet 1) and OH radicals were formed in the reaction of H atoms (inlet 2) with NO_2 (inlet 3). Since reaction (7) forming HOI from $OH + I_2$ is much faster than reaction of OH with HOI, a rapid and complete disappearance of I_2 (in the timescale of OH + HOI reaction) was observed. As a consequence, the experiments for the kinetic study of reaction (2) were carried out in the absence of molecular iodine in the reaction zone. The initial concentrations of HOI and OH radicals were $(3.0–8.0) \times 10^{11}$ and $(2.9–30.6) \times 10^{12}$ molecule cm^{-3}, respectively. The linear flow velocity in the reactor was in the range 900–1400 cm s^{-1}. Rather high concentrations of NO_2 were used in these experiments: $(1.3–1.5) \times 10^{14}$ molecule cm^{-3}. Such an excess of NO_2 was needed in order to scavenge oxygen atoms formed in the OH + OH reaction, which could initiate secondary chemistry and influence the kinetic measurements.

A significant consumption (up to 50% in a few kinetic runs) of the excess reactant, i.e. OH radicals, could be observed. This OH consumption was due to the following processes:

$$OH + HOI \rightarrow IO + H_2O \quad (2)$$

$$OH + IO \rightarrow I + HO_2 \quad (10)$$

$$OH + HO_2 \rightarrow H_2O + O_2 \quad (11)$$

$$OH + OH \rightarrow O + H_2O \quad (4)$$

$$OH + O \rightarrow H + O_2 \quad (12)$$

$$OH + \text{wall} \rightarrow \text{loss} \quad (8)$$

(IO was detected by mass spectrometry as a product of reaction (2) but not quantified in the present study). A major contribution comes from reaction (4), especially at the highest initial concentrations of OH radicals. In order to take into account this consumption of OH, the rate constant of reaction (2) was determined from a numerical simulation of the HOI decay kinetics, using the experimental temporal profiles of [OH]. The results obtained in this series of experiments are presented in Fig. 5: the dependence of the pseudo-first order rate constant of HOI decay, $k'_2 = k_2 \times [OH]$, is shown as a function of the concentration of OH radicals. The linear fit to the data on Fig. 5 provides with the value for the rate constant of reaction (2): $k_2 = (5.0 \pm 0.4) \times 10^{-12}$ cm^3 molecule^{-1} s^{-1}, where quoted uncertainty represents 1 standard deviation.

Secondary chemistry which could affect the HOI decays can be discussed. One reaction that could regenerate HOI in the chemical system used is the reaction of IO with HO_2, IO being the primary product of reaction (2) and HO_2 possibly formed in

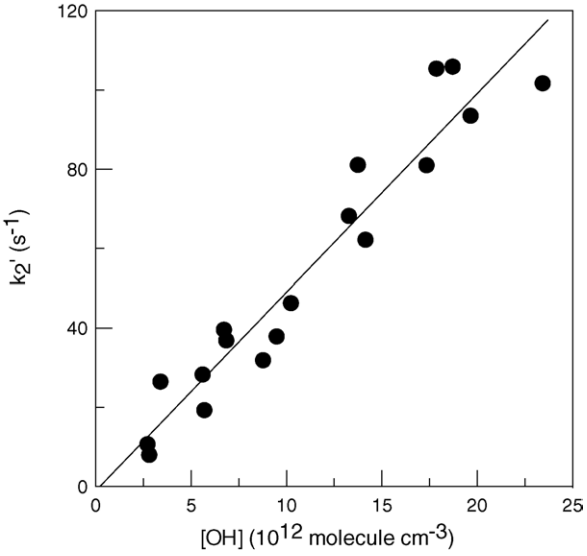

Fig. 5. Pseudo-first order plot of HOI consumption by OH radicals in excess.

the secondary reaction of OH with IO (reaction (10)):

$$HO_2 + IO \rightarrow HOI + O_2 \quad (13)$$

$k_{13} = 7.6 \times 10^{-11}$ cm^3 molecule^{-1} s^{-1} [2]. However, the possible impact of this reaction can be considered as negligible, since steady state concentrations of these species should be very low: both species are scavenged in their rapid reactions with OH (reactions (10) and (11)) and also with NO:

$$HO_2 + NO \rightarrow OH + NO_2 \quad (14)$$

$k_{14} = 8.4 \times 10^{-12}$ cm^3 molecule^{-1} s^{-1} [2];

$$IO + NO \rightarrow I + NO_2 \quad (15)$$

$k_{15} = 1.8 \times 10^{-11}$ cm^3 molecule^{-1} s^{-1} [2]. NO was present in the reactor, since it was formed in the OH source (reaction (3)) and in the sequence of reactions:

$$OH + OH \rightarrow O + H_2O \quad (4)$$

$$O + NO_2 \rightarrow NO + O_2 \quad (16)$$

$k_{16} = 9.9 \times 10^{-12}$ cm^3 molecule^{-1} s^{-1} [2]. Kinetics of HOI decay could be also influenced by the presence of oxygen atoms formed in reaction (4), although once formed, O atoms are mainly removed with OH (reaction (12)) and NO_2. In order to estimate the possible contribution of this reaction to the consumption of HOI, a numerical simulation of the reactive system with a complete reaction mechanism was performed. To our knowledge, the rate constant of the O + HOI reaction is unknown. In the simulations, the value of 10^{-10} cm^3 molecule^{-1} s^{-1} has been used for the rate constant of this reaction, which seems to be realistic considering that the rate constant of the O + HOBr reaction is 3.1×10^{-11} cm^3 molecule^{-1} s^{-1} and that the reaction OH + HOI is much faster than the reaction OH + HOBr for which $k < 5 \times 10^{-13}$ cm^3 molecule^{-1} s^{-1} at $T = 298$ K [5]. Even with such a high value of the rate constant, the contribution of O + HOI reaction to the consumption of HOI was found to be 20% at the maximum under the experimental conditions of the present study.

Finally, the recommended value of k_2 from the present study is:

$$k_2 = (5.0 \pm 1.2) \times 10^{-12} \text{ cm}^3 \text{ molecule}^{-1} \text{ s}^{-1} \quad (T = 320 \text{ K})$$

The uncertainty on k_2 represents the combination of statistical and estimated systematic errors.

4. Discussion

The present study of reactions (1) and (2) is the first to be reported; the obtained results cannot be compared with other ones. HOI is an important atmospheric iodine species formed in the reaction of IO with HO_2. However, the reaction of HOI with the principal atmospheric oxidant, OH radical, has never been studied. The reason for this is that the main fate of HOI in the atmosphere is its photolysis (producing OH and I and with an estimated lifetime lower than 3 min throughout most of the atmosphere [13]). Heterogeneous loss is an another important fate for atmospheric HOI.

The value of the total rate constant measured for reaction (1) can be compared with available kinetic data for reactions of OH radicals with other halogen and dihalogen molecules. In earlier papers [3,4], Loewenstein and Anderson described a correlation between the ionization potentials of the diatomic halogen molecules and their reactivity toward OH radicals. The ionization potential of IBr is 9.98 eV [14] and the rate constant $k_1 = 1.4 \times 10^{-10}$ cm^3 molecule^{-1} s^{-1} measured in the present study for OH + IBr is found to be between those for OH + ICl (IP = 10.31 eV [14], $k = 2.0 \times 10^{-11}$ cm^3 molecule^{-1} s^{-1} [4]) and OH + I_2 (IP = 9.28 eV [14], $k = 2.1 \times 10^{-10}$ cm^3 molecule^{-1} s^{-1} [2]). Thus, the rate constant obtained for reaction (1) is in good agreement with this correlation.

Concerning the mechanistic data obtained in the present study for the OH + IBr reaction, it is interesting to make a comparison with those for analogous reactions of OH radicals with BrCl and ICl. Thermochemical and available mechanistic data for these reactions are presented in Table 1. From an analysis of the OH reactivity toward Cl_2, Br_2 and I_2, Gilles et al. [12] speculated that one would predict the most exothermic channels to be the major product channels of OH reactions with dihalogen molecules. It was noted, in particular, that the thermodynamically favored HOBr forming channel is expected to be the dominant one in the OH + IBr reaction. This expectation is not supported by the results of the present study, HOI being observed as the major reaction product. However, it should be noted at this point that the exothermicity of HOI forming channel (although uncertain, Table 1) is higher than that of HOBr forming channel of reaction (1). The mechanistic data presented in Table 1 seem to indicate that thermochemistry is not the unique factor determining the partitioning of the products of the OH + XY reactions. Another important factor determining the mechanism of XY reactions with radicals (R) seems to be "electronegativity order-

Table 1
Thermochemical and mechanistic data for OH + XY reactions (X, Y = Cl, Br, I)

XY	ΔH_{HOY}[a] (kJ mol^{-1})	ΔH_{HOX}[a] (kJ mol^{-1})	k_{HOY}/k_Σ[b]	k_{HOX}/k_Σ[b]	Reference
BrCl	−14.9 ± 1.9	+8.8 ± 1.6	≤0.13[c]	≈1	[5]
ICl	−22.7 ± 1.7	−3.0 ± 5.9	≈1	≤0.01	[4]
IBr	−31.8 ± 1.6	−37.8 ± 6.0	0.14	0.84	This work

[a] The thermochemical data used for the calculations of ΔH are from reference [1].
[b] Branching ratios for HOX and HOY forming channels.
[c] Calculated from the data of reference [5].

ing rule" discussed in previous papers [3,4,15,16] and stating that approach of R to the less electronegative halogen atom of XY is energetically favored. In the case of OH + XY reactions (where Y is lighter, i.e. more electronegative than X) that would mean that the HOX forming channel should be favored. The experimental data obtained for the reaction of OH with IBr (present study) and with BrCl [5] are in line with this rule.

In conclusion, theoretical calculations are needed to better elucidate the mechanism of the reactions of OH radical with dihalogen molecules. However, an experimental basis for the theoretical calculations should be improved: the existing data (Table 1) need to be confirmed and extended to temperature dependence studies.

Acknowledgement

This study has been performed within the Environment Programme of the European Commission (LEXIS project ENV4-CT95-0013).

References

[1] S.P. Sander, R.R. Friedl, D.M. Golden, M.J. Kurylo, R.E. Huie, V.L. Orkin, G.K. Moortgat, A.R. Ravishankara, C.E. Kolb, M.J. Molina, B.J. Finlayson-Pitts, Chemical Kinetics and Photochemical Data for Use in Stratospheric Modeling, Evaluation No. 14, JPL Publication 02-25, NASA, Jet Propulsion Laboratory, Pasadena, CA, 2003.
[2] R. Atkinson, D.L. Baulch, R.A. Cox, J.N. Crowley, R.F. Hampson, J.A. Kerr, M.J. Rossi, J. Troe, Evaluated Kinetic and Photochemical Data for Atmospheric Chemistry, International Union of Pure and Applied Chemistry (IUPAC), March 2005, web version http://www.iupac-kinetic.ch.cam.ac.uk.
[3] L.M. Loewenstein, J.G. Anderson, J. Phys. Chem. 88 (1984) 6277.
[4] L.M. Loewenstein, J.G. Anderson, J. Phys. Chem. 89 (1985) 5371.
[5] A. Kukui, U. Kirchner, Th. Benter, R.N. Schindler, Ber. Bunsenges. Phys. Chem. 100 (1996) 455.
[6] Y. Bedjanian, G. Le Bras, G. Poulet, J. Phys. Chem. A 103 (1999) 7017.
[7] Y. Bedjanian, G. Le Bras, G. Poulet, Int. J. Chem. Kinet. 31 (1999) 698.
[8] Y. Bedjanian, G. Le Bras, G. Poulet, Chem. Phys. Lett. 266 (1997) 233.
[9] Y. Bedjanian, G. Le Bras, G. Poulet, Int. J. Chem. Kinet. 30 (1998) 933.
[10] F. Kaufman, J. Phys. Chem. 88 (1984) 4909.
[11] T.R. Marrero, E.A. Mason, J. Phys. Chem. Ref. Data 1 (1972) 3.
[12] M.K. Gilles, J.B. Burkholder, A.R. Ravishankara, Int. J. Chem. Kinet. 31 (1999) 417.
[13] D. Bauer, T. Ingham, S.A. Carl, G.K. Moortgat, J.N. Crowley, J. Phys. Chem. A 102 (1998) 2857.
[14] J.L. Franklin, J.G. Dillard, H.M. Rosenstock, J.T. Herron, K. Draxl, F.H. Field, Ionization Potentials, Appearance Potentials, and Heats of Formation of Gaseous Positive Ions, U.S. Department of Commerce, Washington, DC, 1969.
[15] D.D. Parrish, D.R. Herschbach, J. Am. Chem. Soc. 95 (1973) 6135.
[16] D.R. Herschbach, Faraday Discuss. Chem. Soc. 55 (1973) 233.